SolarPACES 2023, 29th International Conference on Concentrating Solar Power, Thermal, and Chemical Energy Systems

Measurement Systems, Devices, and Procedures

https://doi.org/10.52825/solarpaces.v2i.756

Published: 16 Sep. 2024

Robust Deflectometry

Braden Smith[1] and Randy Brost[1]

[1] Sandia National Laboratories, USA

*Correspondence: Braden Smith, bsmith4@sandia.gov

Abstract. Concentrating Solar Power (CSP) mirrors must have high slope accuracy in order to achieve high solar concentration. Deflectometry is an established method for measuring high-resolution, high-accuracy maps of mirror slope. In this paper we describe improvements to Sandia's deflectometry system, SOFAST, which enable it to be accurately calibrated even in difficult conditions of poor access to system components, imperfect components, and varying ambient light. These extensions improve the robustness of the system and expand the range of problems it can solve.

Keywords: Deflectometry, Optical Metrology, SOFAST, Concentrating Solar Power, Robust

1. Introduction

Concentrating solar power (CSP) mirrors are often physically large and can have focal lengths of up to hundreds of meters, which corresponds to small surface curvature. Deflectometry is an effective CSP metrology tool, because it can handle large sized mirrors and can resolve the very small curvatures typically found in CSP heliostat mirrors [1, 2, 3].

Deflectometry works by displaying an image with known dimensions and viewing the reflection of this pattern with a machine vision camera. The deflectometry system interprets the distortion of the pattern in the reflected image as curvature of the mirror. However, since CSP metrology requires high accuracy to resolve the small amounts of surface slope (sometimes less than 1 milliradian), accurately calibrating the deflectometry system is a crucial step of deployment.

We seek a robust deflectometry system which can be set up quickly in a variety of locations while maintaining ease and accuracy of calibration. Such a system can support applications requiring a temporary setup, a site with changing conditions, or in a location with other non-ideal conditions. For example, a deflectometry system with a robust calibration procedure benefits factory environments where setups often evolve and lighting conditions cannot be strictly controlled. Another example is using deflectometry outdoors to measure a solar field by using the solar tower as a projector screen, as demonstrated by [4, 5]. The screen surface is likely not flat, likely not uniformly reflective, and inaccessible to directly measure. Additionally, in some situations the deflectometry system may interfere with field operations and must be set up quickly in a single night.

Sandia's deflectometry tool, SOFAST, began as a stationary installation used for laboratory measurements and outdoor measurement of dish collectors [6]. We have since improved the robustness of SOFAST by adding features that improve the accuracy and speed of the SOFAST calibration procedure. This improved robustness has allowed us to use

SOFAST in environments previously not suitable for SOFAST. Deflectometry systems that can accommodate non-ideal conditions and produce accurate results can be used in a wider range of metrology applications.

2. Improved Robustness of SOFAST

2.1 Camera lens calibration

Robust deflectometry systems require camera lens distortion calibration techniques that minimize calibration time while maintaining calibration accuracy. Fast camera calibrations enable new systems to be stood up faster and system modifications to be completed faster. However, we have found that errors of just a few percent in camera calibration parameters can cause errors of up to several tenths of a milliradian in reported surface slope in our systems.

Typically, camera distortion is characterized by taking many images of a regular pattern, such as a black and white checkerboard [7]. These images are fed into an algorithm that solves for camera focal length and fits the residual lens distortion to a polynomial surface defined by a series of distortion coefficients [7]. A typical checkerboard and an example distortion map are shown in Figure 1.

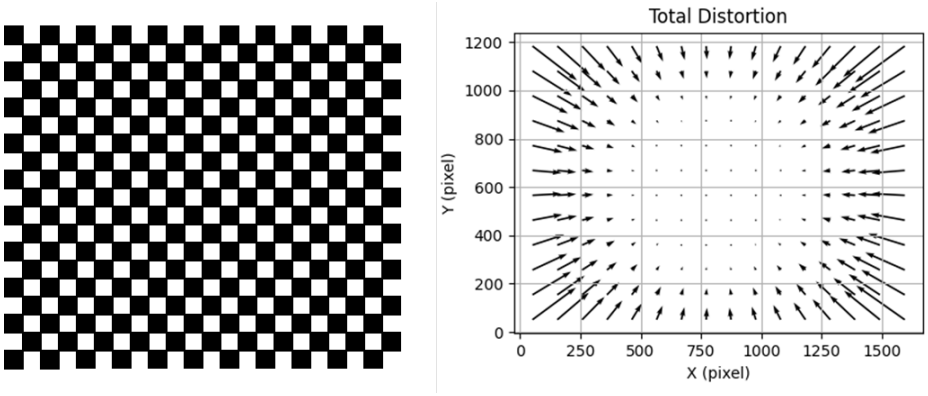

Figure 1. *Typical checkerboard target and example distortion map of Sandia's 50mm lens.*

To increase calibration efficiency by reducing the number of and increasing the fidelity of calibration images, we developed a simulation tool that informs the required checkerboard flatness, the ideal range of checkerboard-camera angles, and sufficient number of captured images given the current setup geometry. The provided recommended calibration parameters increase the efficiency and reliability of camera calibrations.

A full list of the parameters we used in our example simulation is shown in Table 1; these correspond to calibrating a Basler acA1600-20gm camera with a 50mm lens. Checkerboard flatness is defined as the peak-to-valley height variation of a spherically curved checkerboard and the checkerboard-camera angle is measured between the camera optical axis and checkerboard normal.

Table 1.

Checkerboard y number	19 squares
Checkerboard x number	22 squares
Checkerboard y dimension	0.95 meters
Checkerboard x dimension	1.1 meters
Camera nominal focal length	14493 pixels

Number of trials to compute average and standard deviation	50
Nominal checkerboard to camera distance	13 meters
Checkerboard corner location uncertainty	0.5 pixels STDEV

Figure 2 shows the average and standard deviation of the reported focal length for each parameter sweep in our simulation, with checkerboard flatness being most sensitive. These graphical outputs inform the user of requirements for a desired calibration accuracy.

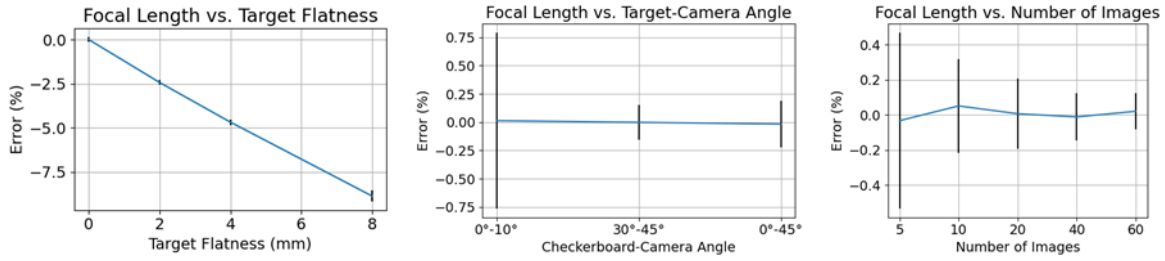

Figure 2. *Calculated focal length error for parameter sweeps of target flatness, target-camera angle, and number of total images taken. Error bars represent two standard deviations.*

2.2 Screen flatness and distortion

Deflectometry also relies on knowing the (*x*,*y*,*z*) location of each point of the displayed pattern. Measuring this can be especially difficult if using a projector, as projector lens distortion, non-normal incidence of the projector and screen, and variations in screen surface flatness affect the locations of the screen points. In some instances, using a projector/screen setup is the only feasible way to create a deflectometry system, and flat screen surfaces are not always available.

To improve the efficiency and accuracy of calibration when setting up SOFAST instances, we developed a photogrammetric screen mapping tool. The tool works by displaying a series of sinusoidal fringes on the screen which are captured by a calibrated machine vision camera from several angles. The fringes vary from coarse to fine frequency, for both horizontal and vertical directions. An algorithm then calculates the shape of the screen using photogrammetry calculations based on the images. This calibration step is easily done by one person in under 20 minutes.

Figure 3 shows the measurement of one of Sandia's SOFAST screens. To cross check the measurements, the same section of wall was measured with a FARO LIDAR scanner. With this screen configuration, the two methods agreed within ~1mm.

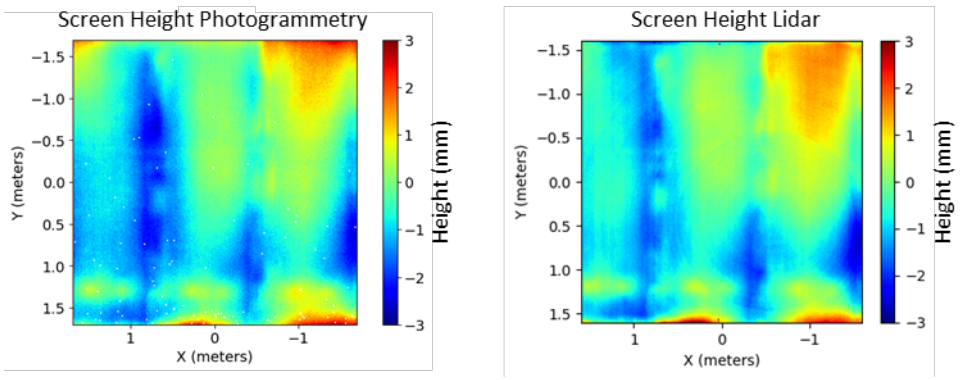

Figure 3. *Comparison of screen height measurements using photogrammetry method and FARO lidar scanner.*

2.3 Component position calibration

Deflectometry systems need to know the relative position of the components, such as the mirror, points on the screen, and camera. This calibration needs to be completed every time a new system is set up or modified. In a robust deflectometry system, this measurement is made quickly and accurately and does not require physical access to the screen or camera. This is important for deflectometry systems, because screen and camera locations can be in physically inaccessible locations.

To quickly and accurately perform this calculation when setting up SOFAST instances, we developed a photogrammetric method of measuring the camera and screen poses using Aruco markers. Aruco markers are binary black/white patterns that can be easily found and identified with machine vision cameras [8]. We placed Aruco markers in the field of view of the camera and around the screen. The markers placed around the screen perimeter are placed to intersect with the screen's xyz axes, thus defining the xyz location of the screen. Another calibrated machine vision camera captures many images of the scene from different angles and, through photogrammetry, the relative positions of the markers is calculated. Once the markers are located, the camera can easily be located relative to the markers. The camera location is determined by using the camera to capture an image including the Aruco markers, which are now in known locations. Figure 4 shows our experimental setup when calibrating Sandia's SOFAST system.

Initial tests have shown that the position and orientation of the screen and camera can be calculated by one person in one day with the screen and camera in inaccessible locations. The accuracy of the photogrammetric method has been shown to be comparable to a manual "by hand" measurement. Future work will focus on further improving accuracy and validation.

Figure 4. *Example of photogrammetric component calibration measurement setup.*

2.4 Ambient light control

Deflectometry systems measure visual patterns; thus, they are susceptible induced errors from external light sources. A robust deflectometry system comes with a set of lighting guidelines and/or can calculate when ambient lighting conditions are too bright. This adds value to a deflectometry system by allowing it to be installed in locations where lighting is not strictly controlled, such as factory or other locations with varying ambient light.

To improve the robustness of SOFAST, we characterized the range of acceptable fringe contrast. We ran multiple SOFAST data collects with increasing ambient light levels and noted the change in the calculated slope map from nominal. For each light level, SOFAST reported the fringe contrast, shown in Equation (1), where I is the signal as seen by the camera.

$$Contrast = \frac{I_{max} - I_{\min}}{I_{max} + I_{min}} \quad (1)$$

Figure 5 shows ambient light-induced slope error as a function of fringe contrast using Sandia's SOFAST installation. This result provides the user a recommendation of how much ambient light is acceptable for a target accuracy.

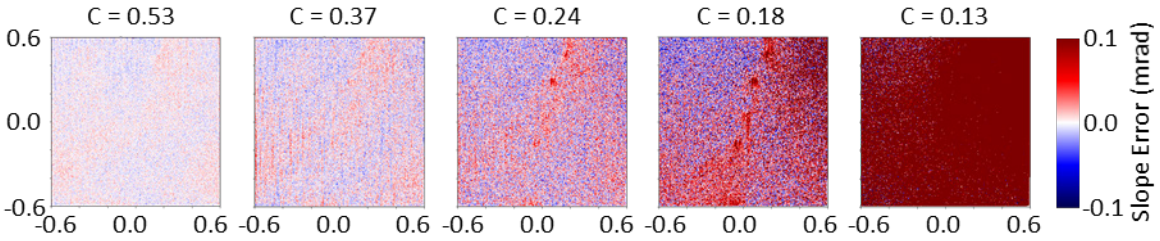

Figure 5. *Induced SOFAST slope error for different contrast values C, while measuring a National Solar Thermal Test Facility heliostat facet.*

2.5 Screen brightness nonuniformity

A robust deflectometry system can also operate when the screen does not have uniform reflectance or illumination or the camera does not have uniform throughput. Since the response between projector and camera is not usually linear, variations in the screen reflectance can cause errors in the calculations if the system uses projected fringes, such as SOFAST described in [1]. Mobile deflectometry systems benefit from not relying on a highly uniform, white screen, as these may not always be available. This also enables a wider range of lenses to be used, such as lenses with high amounts of vignetting.

We improved the way SOFAST handles nonuniformity in screen brightness by including a screen-camera response calibration step. The calibration works by mapping the relationship between the brightness commanded to the projector and the pixel value read by the camera. We scale this mapping per-pixel depending on the relative response of each pixel. Figure 6 shows the shape of ideally sinusoidal fringes as captured by the camera and after calibration.

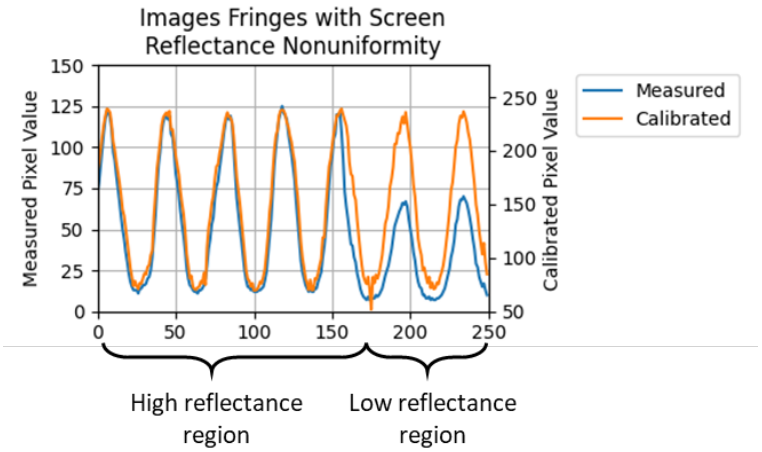

Figure 6. *Sinusoidal fringes projected onto a screen with nonuniform reflectance, before and after pixel calibration.*

3. Conclusion

CSP metrology can benefit from robust deflectometry tools that can be accurately calibrated in a variety of non-ideal conditions. We have discussed improvements made to Sandia's deflectometry tool, SOFAST, that improve its robustness. These improvements have given SOFAST more utility and allow SOFAST to make measurements in scenarios previously not possible due to time constraints or location constraints.

Data availability statement

Both the data and code reported in this paper are publicly available in OpenCSP. Send inquiries to OpenCSP@sandia.gov.

Author contributions

Randy Brost contributed conceptualization, investigation, formal analysis, software, funding acquisition, project administration, and writing. Braden Smith contributed software, data curation, formal analysis, investigation, and writing.

Competing interests

The authors declare no competing interests.

Acknowledgement

We would like to thank Anthony Evans, Roger Buck, and Robert Crandell of Sandia National Laboratories for their help with data collection and design. Sandia National Laboratories is a multi-mission laboratory managed and operated by National Technology & Engineering Solutions of Sandia, LLC, a wholly owned subsidiary of Honeywell International Inc., for the U.S. Department of Energy's National Nuclear Security Administration under contract DE-NA0003525. This written work is authored by an employee of NTESS. The employee, not NTESS, owns the right, title and interest in and to the written work and is responsible for its contents. Any subjective views or opinions that might be expressed in the written work do not necessarily represent the views of the U.S. Government. The publisher acknowledges that the U.S. Government retains a non-exclusive, paid-up, irrevocable, world-wide license to publish or reproduce the published form of this written work or allow others to do so, for U.S. Government purposes. The DOE will provide public access to results of federally sponsored research in accordance with the DOE Public Access Plan.

References

[1] C. E. Andraka, et. al., "Rapid Reflective Facet Characterization Using Fringe Reflection Techniques," Proceedings of Energy Sustainability 2009, ASME.

[2] T. März, et al. Validation of Two Optical Measurement Methods for the Qualification of the Shape Accuracy of Mirror Panels for Concentrating Solar Systems. Journal of Solar Energy Engineering 133, August 2011.

[3] CSP Services. QDec system. https://www.cspservices.de/wp-content/uploads/CSPS-QDec.pdf.

[4] S. Ulmer, T. März, C. Prahl, W. Reinalter, B. Belhomme. Automated high resolution measurement of heliostat slope errors. Solar Energy 85, pp. 685-687, 2011.

[5] R. Brost, B. Smith, F. Brimigion. Agile Deflectometry. Presented in SolarPACES 2022.

[6] C. E. Andraka, et al. AIMFAST: Initial Dish System Alignments Results Using Fringe Reflection Methods. Proceedings of ASME 2011 5th International Conference on Energy Sustainability. 2011.

[7] OpenCV. https://docs.opencv.org/4.x/dc/dbb/tutorial_py_calibration.html.

[8] S. Garrido-Jurado, et. al., “Automatic generation and detection of highly reliable fiducial markers under occlusion,” Pattern Recognition, vol. 47, no.6, pp. 2280-2292, 2014, https://doi.org/10.1016/j.patcog.2014.01.005.